Journal of Power Sources 245 (2014) 487–494

Contents lists available at SciVerse ScienceDirect

Journal of Power Sources

journal homepage: www.elsevier.com/locate/jpowsour

Sulfonated silica-based fuel cell electrode structures for low humidity applications

Jennie I. Eastcott, E. Bradley Easton*

Faculty of Science, University of Ontario Institute of Technology, 2000 Simcoe Street North, Oshawa, Ontario, Canada L1H 7K4

HIGHLIGHTS

- Sulfonated silica ceramic carbon electrodes (SS-CCE) were tested as PEM fuel cell cathodes.
- Nafion-based cathodes were also tested.
- Nafion-based cathodes severe performance losses when with cathode gas feed RH drops below 60%.
- SS-CCE cathodes showed no change in performance when cathode gas feed RH was decreased down to 20%.
- SS-CCE performance stability arises from enhanced water retention & redistribution in the MEA.

GRAPHICAL ABSTRACT

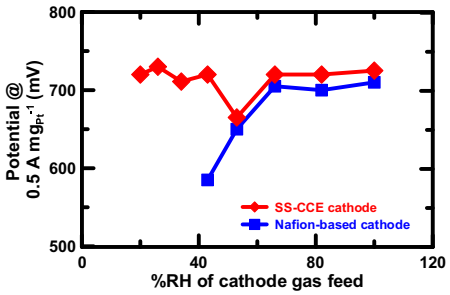

ARTICLE INFO

Article history:
Received 17 March 2013
Received in revised form
29 June 2013
Accepted 1 July 2013
Available online 9 July 2013

Keywords:
PEM fuel cell
Ceramic carbon electrode
Sol–gel
Relative humidity
Water management
Carbon-supported catalysts

ABSTRACT

Ceramic carbon electrodes (CCEs) are prospective candidates for use in proton exchange membrane fuel cells due to their high surface area, water retention properties, and durable nature. We have determined that incorporating small amounts of sulfonated silane in the CCE structure can lead to a profound enhancement of catalytic activity and proton conductivity. To evaluate the usefulness of a new catalyst layer for practical use, performance of the materials under various conditions must be considered. We have compared the properties of membrane electrode assemblies (MEA) prepared with CCE cathode catalyst layers to that of an MEA prepared with Nafion-based cathode catalyst layers. The MEAs were characterized via transmission electron microscopy, thermogravimetric analysis, infrared spectroscopy, and BET analysis. Fuel cell performance using different cathode gas relative humidity (RH) feed conditions was monitored using electrochemical impedance spectroscopy and polarization curves. Our CCE cathode materials maintained stable performance and had improved water management capabilities at low relative humidities, whereas Nafion-containing cathodes have performed poorly. The enhanced performance and tolerance to low RH is explained in terms of water retention within the CCE-based MEA.

© 2013 Elsevier B.V. All rights reserved.

1. Introduction

The energy requirements of modern civilization are rapidly consuming our natural resources, and society must look at alternatives to fossil fuels in order to maintain current output and satisfy energy demand. Proton exchange membrane fuel cells (PEMFCs) are one technology with the potential to help meet both current and future energy needs [1]. The heart of a PEM fuel cell is the membrane electrode assembly (MEA) which consists of anode and cathode electrodes separated by a proton exchange membrane. Typical commercial catalyst layers contain a carbon-supported platinum catalyst combined with Nafion® ionomer

* Corresponding author. Tel.: +1 905 721 8668x2936; fax: 1 905 721 3304.
E-mail address: Brad.Easton@uoit.ca (E.B. Easton).

0378-7753/$ – see front matter © 2013 Elsevier B.V. All rights reserved.
http://dx.doi.org/10.1016/j.jpowsour.2013.07.005

[2]. The role of the ionomer is two-fold, as it supplies proton conductivity to the catalyst layer to increase catalyst utilization [3] as well as bind the carbon support. Several ionomers are commercially available but suffer from shortcomings such as high cost [4], restriction of gas pores [5], and poor performance in low water environments (low relative humidity and high temperature) [6]. Reduction or replacement of Nafion® and other perfluorosulfonic acid ionomers in the catalyst layer is essential to diminish these issues. The use of surface-modified carbon supports has been shown to be a somewhat effective method reducing catalyst layer Nafion® content [5,7–13]. Hydrocarbon-based ionomers such as sulfonated poly(ether ether ketone) (SPEEK) [4,14–18], sulfonated polyphosphazene [19], and poly sulfones [20] have been explored as Nafion® replacements but each one has its own unique set of challenges to be conquered.

Another approach to improving catalyst layer performance is by modification of the electrode support structure [21]. Electrodes are generally prepared by mixing Pt-supported carbon and Nafion ionomer solution without any additional treatment, which does not ensure suitable access to platinum particles throughout the catalyst layer. Several methods of electrode modification include use of organic-inorganic hybrid materials [22–25] to improve the accessibility to platinum and, in turn, the abundance of triple-phase sites. Ceramic carbon electrodes (CCEs) are promising candidates for fuel cell electrodes in this regard. The tuneable nature of CCEs makes them suitable candidates for use in a number of energy applications such as fuel cells [26–28], sensors [29,30], hydrogen production [31–33], and supercapacitors [34,35]. CCEs consist of electronically conductive carbon particles bound by a ceramic binder prepared via the sol–gel process to produce a gel from colloidal suspensions [36]. The sol–gel synthetic method allows for numerous conditions (e.g. pH, solvent, concentration) to be varied in order to modify material properties such as microstructure. The ceramic component is chosen to provide specific properties dependent upon the desired application. Our previous research demonstrated that introduction of the hydrophilic SiO_2 backbone affects the proton conductivity of CCEs without the addition of a functionalized side chain [27]. We have since incorporated an organosilane which has sulfonic acid moieties and hygroscopic properties to allow for enhanced proton conduction and water retention [37].

Water is essential to facilitate good proton conduction, and as such, the ability to retain water is imperative for MEA function at high temperatures (>80 °C) and low relative humidity conditions. Electrodes containing Nafion require hydration to ensure optimal performance [25], which limits the operating conditions of the MEAs. Additionally, extra power is required to maintain humidified gas flows [25]. Thus, it is desirable to operate a fuel cell under lower humidity conditions, but the maintenance of a water balance in the MEA can be a difficult task. Too little water in the membrane can hinder proton conductivity while excess water can flood the catalyst layer and limit gas transport [25,38]. In order to operate in dry environments, the MEA requires a mechanism to maintain moisture content [39]. Excess water at the cathode can result in back-diffusion of water from the cathode across the membrane to alleviate flooding by minimizing the water concentration gradient [38]. Therefore, it is possible that under low humidity conditions, water in the catalyst layer could aid in membrane hydration [39]. In this work, an organosilane precursor with sulfonic acid groups has been used to increase proton conduction within CCEs. The hygroscopic properties of the chosen organosilane not only ensure good hydration within the catalyst layer but may promote membrane hydration via back-diffusion. Nafion, by contrast, is known to be at peak performance when fully hydrated and conductivity decreases with reduced water content [39]. Our fabrication method involves adding the organosilane precursors to the carbon in monomer form and initiating polymerization [37]. Polymerization *in situ* allows the organosilane to chemically bond to surface hydroxyl groups on the carbon support to facilitate efficient proton transport.

We have previously demonstrated that sulfonated silane-CCE (SS-CCE) fuel cell cathodes outperform SiO_2-based CCE cathodes [40] and can perform on par with Nafion-based cathodes at 80 °C using fully humidified gases [27], conditions where Nafion-based MEAs perform at their best. This performance was explained in terms of the high water retention and proton conductivity using sulfonated silica-based ionomers. Here, we report the dependence of fuel cell performance of SS-CCE cathodes on the low relative humidity (RH) of the cathode gas feed. The results have been compared to the performance of a commercial Nafion-based cathode under the same conditions. The hygroscopic nature of the silicate material in the electrodes appears to provide a mechanism for water retention within the MEA that is normally tailored within the membrane. Water retention in the catalyst layer may provide a source of hydration for the membrane at low RH via back-diffusion of water, while ensuring flooding of the membrane pores at higher RH is minimal.

2. Experimental

2.1. CCE preparation

CCE materials for spray deposition were prepared at via the sol–gel method as outlined in our previous publications [37,40]. Briefly, dry 20% Pt on Vulcan XC72 carbon black (ETEK BASF) was combined with deionized water, methanol, and 6 M ammonium hydroxide. Deionized water was added first to prevent platinum ignition upon subsequent addition of methanol. The catalyst mixture were mechanically stirred, after which additions of tetraethylorthosilicate (TEOS) and 3-(trihydroxysilyl)-1-propanesulfonic acid (TPS, 30–35% in water) were added drop-wise to achieve a 5:95 TPS-to-TEOS mole ratio at a constant total silane concentration of ca. 40%, which was previously determined to be optimal for fuel cell performance.[27,40] After several days, the partially gelled CCE was spray deposited onto a gas diffusion layer (GDL) using an air brush. Following deposition, the resulting electrodes was dried for 30 min at both room temperature and 135 °C. The electrode had a platinum loading of 0.34 mg cm^{-2} and a total silicate loading of 40 wt%, and will be referred to as SS-CCE.

2.2. Materials characterization

Thermogravimetric analysis (TGA) was performed using a TA Instruments Q600 SDT thermal analyzer. Samples were heated from room temperature to 800 °C at a rate of 20 °C min^{-1} under flowing air (50 mL min^{-1}), which enables the determination of the weight percent of the individual components [27,32,41]. Based on this, SS-CCE had an overall silicate content of 40 wt%, of which 6 mol% was TPS (balance TEOS), and 60 wt% platinized carbon. Further details of the thermal analysis behavior of these materials are reported elsewhere [40].

Fourier-transform infrared (FTIR) spectroscopy was performed (PerkinElmer Spectrum 100 FTIR) to verify the presence of sulfonic acid groups with KBr pellets at room temperature. Brunauer–Emmett–Teller (BET) surface areas and pore size data was collected using a Micrometrics ASAP 2020 V4.00 physisorption analyzer. Transmission electron microscopy (TEM) images of the E-TEK catalyst material and the CCE layer were acquired using a Philips CM 10 instrument equipped with an AMT digital camera system.

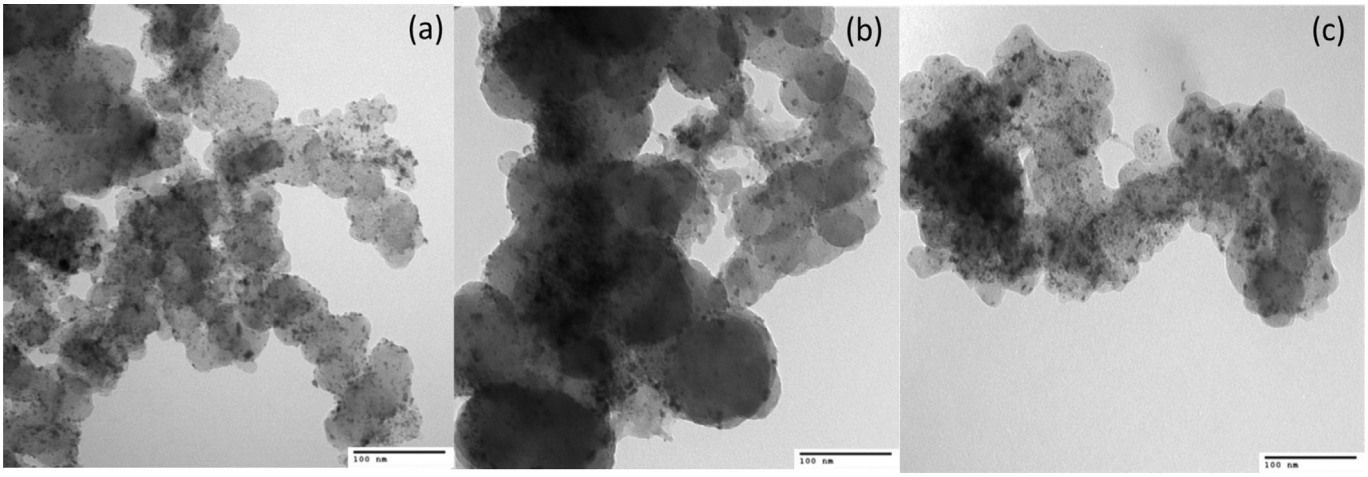

Fig. 1. TEM images of a) as-received E-TEK 20% Pt on Vulcan Carbon, b) sprayed TPS/TEOS CCE catalyst layer, and c) sprayed E-TEK 20% Pt on Vulcan Carbon + 31.5% Nafion.

2.3. Electrochemical measurements

Fuel cell membrane electrode assemblies (MEAs) were fabricated by hot-pressing (150 kg cm^{-2} for 90 s at 130 °C) a 5 cm^2 test electrode (cathode) and a similar-sized commercial anode (ELAT A6STDSIV2.1 Pt loading = 0.5 mg cm^{-2}, proprietary ionomer loading) across a Nafion NRE212 membrane. For comparison, a MEA was prepared using an ELAT electrode as both the test electrode and the anode. MEAs were tested in a 5 cm^2 test fuel cell (Fuel Cell Technologies). Fuel cell testing was performed at a cell temperature of 80 °C with feed gases (H_2 and O_2) pressurized to 10 psig (170 kPa) at the outlets. Gases were humidified by passing them through heated humidifier bottles (Nuvant Systems Inc.) prior to entering the cell. The relative humidity levels of the gas feeds were controlled by varying the temperature of the gas humidifiers with respect to the cell temperature. In all cases, the anode humidifier bottles were maintained at 80 °C in order to maintain 100% RH at the anode inlet. The temperature of cathode humidifier bottles were varied between 45 °C and 80 °C in order to yield 20–100% RH at the cathode inlet.

Electrochemical impedance spectroscopy (EIS) measurements were collected at the aforementioned temperatures with humidified N_2 flowing at the cathode and with the H_2 electrode serving as both the reference and the counter electrode. All electrochemical measurements were performed using a Solartron 1470E Multichannel Potentiostat and a 1260 frequency response analyzer controlled using Multistat software (Scribner Associates). Impedance spectra were collected over a frequency range of 100 kHz to 0.1 Hz at a DC bias potential of 0.425 V. EIS data was analyzed using a finite transmission-line model developed by the Pickup group [42,43].

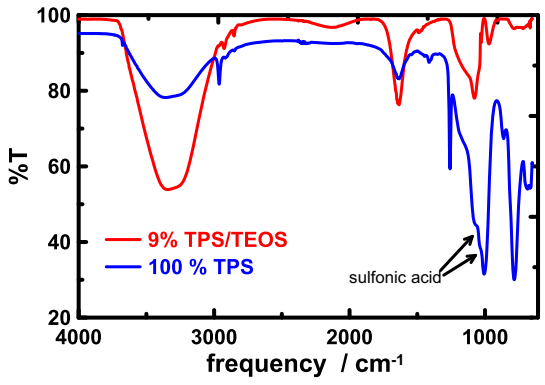

Fig. 2. Comparison of pure TPS and composite TPS/TEOS gels to identify the presence of sulfonic acid functional groups.

3. Results

3.1. Materials characterization

TEM images of catalyst layers are shown in Fig. 1 (180 000× magnification) and compare the as-received Pt/Vulcan catalysts (a) to the SS-CCE catalyst layer (b) as well as a Nafion-bound Pt/Vulcan catalyst layer (CL) (c). Fig. 1 indicates that our spray deposition technique has not resulted in blocking of platinum particles and the catalyst material has not been significantly altered by our procedure. Additionally, little particle or ionomer agglomeration was present in our SS-CCE sample. The SS-CCE catalyst layer (b) did not look considerably different from the Nafion-based layer (c).

The presence of sulfonic acid groups was verified through FTIR spectroscopy. Fig. 2 illustrates the similarities between a gelled sample of TPS and a gelled silicate composite (no Pt/C) containing both TEOS and a small amount of TPS (9%). The FTIR shows the peaks associated with sulfonated functional groups (1030–1070 cm^{-1}) are present in both samples despite the predominance of the TEOS in the composite gel. Through the gelation process, there is no loss of sulfonate functional groups.

Table 1 shows the BET surface area data obtained for SS-CCE material as well as a control sample that contained only TEOS (SiO_2-CCE), but with the same total silane concentration as the SS-CCE sample. The BET analysis indicated the SS-CCE had a surface area of 403 m^2 g^{-1} while the TEOS control had a surface area of

Table 1
Summary of BET data for 45% SiO_2-CCE TEOS control and 4% TPS SS-CCE.

	SiO_2-CCE	SS-CCE
Silane content	45% TEOS	4% TPS (40% silane)
Single point SA (m^2 g^{-1})	394.86	396.57
BET SA (m^2 g^{-1})	404.69	403.14
Total pore volume (cm^3 g^{-1})	0.433	0.263
Volume between 17 and 3000 Å (cm^3 g^{-1})	0.329	0.16
Average pore width (Å)	42.82	26.05
Average pore diameter (Å)	66.76	44.18
Median pore width (Å)	11.02	10.6

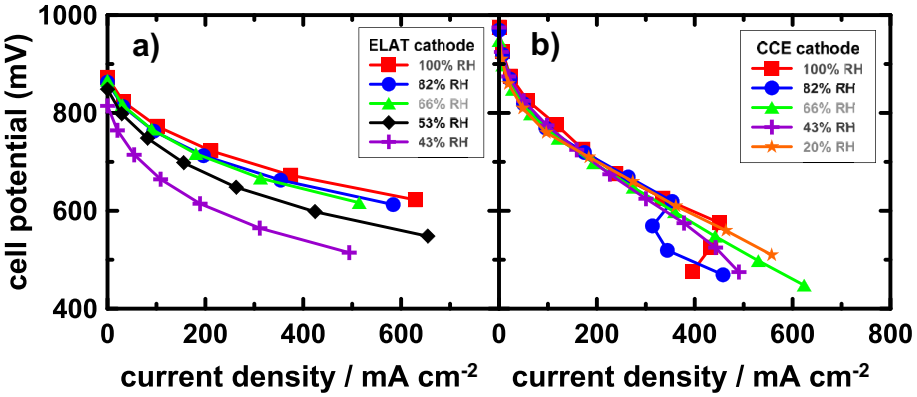

Fig. 3. Comparison of the H_2/O_2 fuel cell polarization curves obtained for (a) ELAT and (b) SS-CCE cathode catalyst layers at multiple cathode feed gas RH levels.

405 $m^2\ g^{-1}$. This suggests that our CCE catalyst layer is a highly porous medium with a surface area that is substantially larger than that of the bare Vulcan carbon surface (250 $m^2\ g^{-1}$, manufacturer's specifications). Addition of a small amount of sulfonated silane has not significantly affected the overall surface area of the CCE material, but has changed the porosity profile. The pore volume and average pore size have been reduced in the SS-CCE compared to the TEOS-only sample. The presence of the sulfonated side chain on the silicate backbone is likely the cause of this reduction, resulting in a higher degree if microporosity compared to the unsulfonated sample.

3.2. Fuel cell electrochemical characterization

The fuel cell performance for CCE catalyst layers under standard conditions was evaluated previously [27,37] in comparison to Nafion-based cathodes. Those electrodes prepared without sulfonic acid groups did display some performance capabilities but they were far below that of Nafion-based electrodes [27]. Electrodes prepared with sulfonated silane precursors were found to have similar performance to Nafion-based electrodes [37]. The impact of the sulfonate groups on the catalyst layer performance is further illustrated in the Supplementary data.

The SS-CCE cathodes appeared to suffer from mass performance losses due to flooding at 100% RH, indicating that the electrodes may be sensitive to high humidity conditions. The effect of relative humidity on fuel cell performance for both the ELAT and SS-CCE cathode catalyst layers is shown in Fig. 3. Measurements were conducted with a constant anode and cell temperature of 80 °C and 100% RH but variable relative humidity at the cathode. At low current densities, the performance of the SS-CCE cathode was superior to the Nafion-based cathode regardless of the relative humidity. Mass transport limitations are evident for the SS-CCE cathode at 100% and 82% RH, indicating that a significant amount of flooding is a concern under these conditions. Since the SS-CCE is a hydroscopic material, the incidence of flooding under fully (or almost fully) hydrated conditions is not surprising. As the %RH continues to decrease, these mass transport losses are no longer evident and the SS-CCE cathode displays no change in performance down to 20% RH. The Nafion-based ELAT cathode had sizeable performance drops when the cathode relative humidity was decreased. Furthermore, the Nafion-based ELAT electrode could not be operated in a stable manner below 43% RH. This is exceedingly evident in Fig. 4, in which the performance has been normalized for the amount of platinum at the cathode. The retention of fuel cell performance at low RH for our CCE catalyst layers is noteworthy. This is important not only because it allows the fuel cell to be operated in multiple environments but also because low humidity conditions aid in the reduction of the overall balance-of-plant. Power is required to humidify the gases to 100% RH, therefore the reduction in gas humidification reduces the amount of parasitic power required for the fuel cell system. Furthermore, real world operation of PEM fuel cells often results in RH conditions inside the catalyst layer that differ drastically from that of the feed gas. Thus, the fact that the CCE performance showed no variation in performance with cathode feed RH indicates that these CCEs would be highly tolerant to transient fluctuations of RH within the catalyst layer.

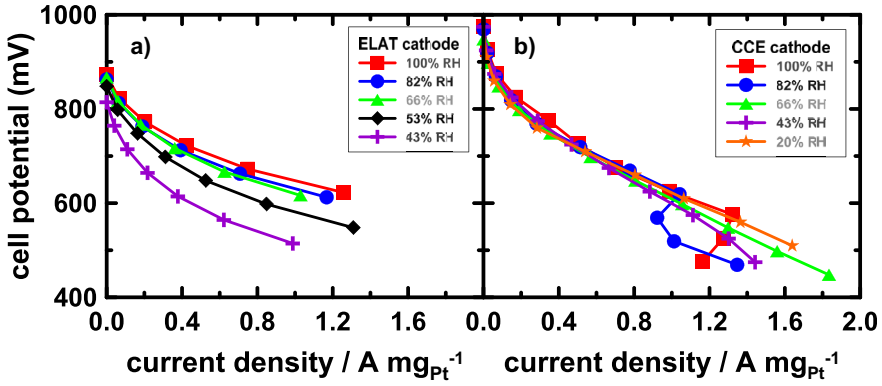

Fig. 4. Comparison of the H_2/O_2 fuel cell polarization curves obtained for (a) ELAT and (b) SS-CCE cathode catalyst layers at multiple cathode gas feed RH levels. Plots have been normalized for platinum loading.

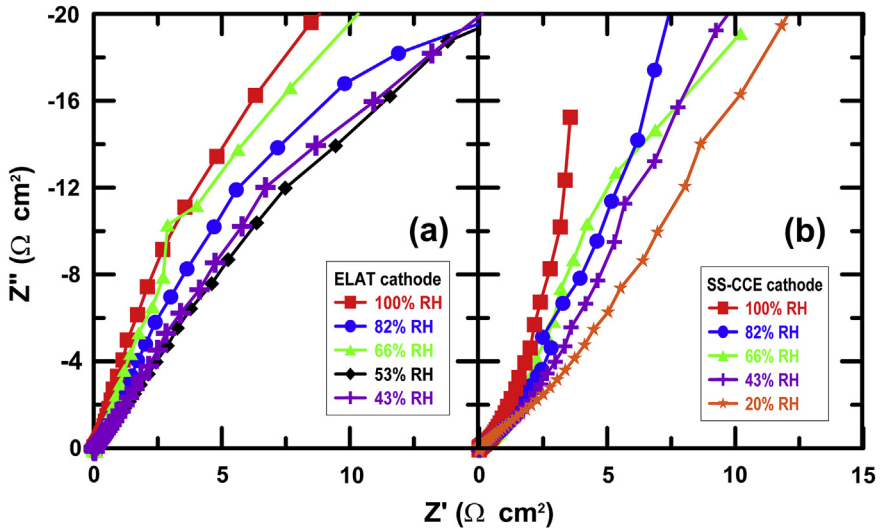

Fig. 5. Nyquist plots of fuel cell EIS data for a) ELAT cathode and b) SS-CCE cathode at 80 °C obtained for multiple cathode gas feed RH levels.

To further evaluate the catalyst layer and determine the mechanism of our CCE's exceptional performance at low relative humidity, additional electrochemical studies were conducted. EIS analysis is a technique that can provide information about changes in conductivity and resistance in the catalyst layer under different conditions, as well as insight into degradation mechanisms [44]. EIS data was analyzed using Nyquist plots (Fig. 5) to monitor changes in ionic resistance. The length of the Warburg region increased as the RH at the cathode decreased for both the ELAT and SS-CCE cathodes, indicating an increase in ionic resistance with lower relative humidity. This is even more evident in an expansion of the high-frequency region (Fig. 6) and is further demonstrated in Fig. 10. As water aids in the conduction of protons, it is not surprising that ionic resistance in the catalyst layer will increase with reduced water content. Capacitance plots in Fig. 7 display this more prominently, as the initial steepness of the capacitance curves decreased with relative humidity for both samples. This trend is highlighted with the expansion of the high-frequency region shown in Fig. 8. Fig. 7 also shows that the SS-CCE cathode has a much higher limiting capacitance, and thus electrode active area [43], above 66% RH. The ELAT cathode displays very little change in limiting capacitance with relative humidity, but the limiting capacitance decreased for the SS-CCE with lower %RH. The limiting capacitance values for each %RH for the ELAT and SS-CCE cathodes were compared in Fig. 9a; also shown in Fig. 9b is the variation in cell potential at a fixed current density of 0.5 A mg_{Pt}^{-1} as a function of RH. While there appears to be an overall decrease in limiting capacitance for the SS-CCE, at as low as 43% RH the limiting capacitance values for both the ELAT and SS-CCE cathodes are comparable. Furthermore, this decrease in limiting capacitance with RH in the SS-CCE, which is correlated with active area [43], seems to have no impact on cell performance as the cell potential at 0.5 A mg_{Pt}^{-1} at 20% RH is almost identical to that at 100% RH. Whereas the Nafion-based ELAT electrode maintains a relatively stable limiting capacitance with varying RH but exhibited a marked decrease in performance below 60% RH.

To examine this further, the EIS data was further analyzed to extract both the membrane resistance, R_{mem}, and the ionic

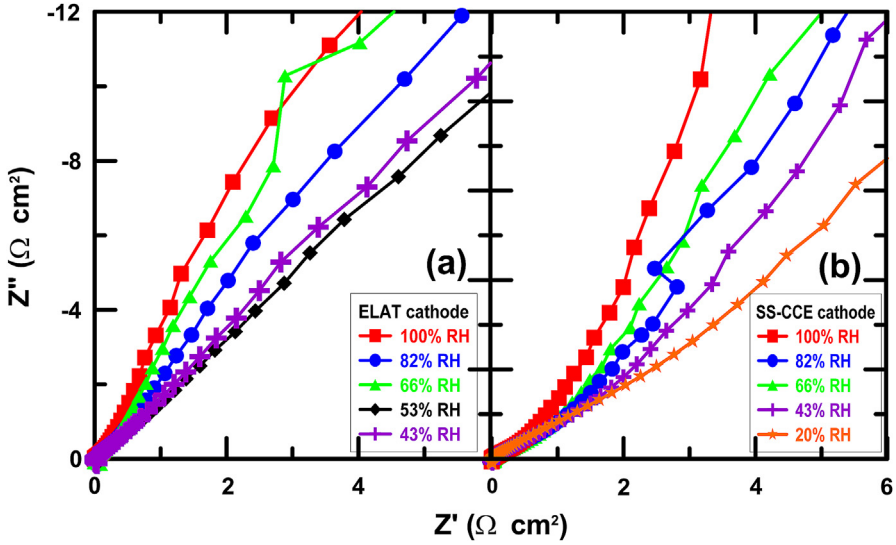

Fig. 6. Expansion of the high-frequency region for Nyquist plots of fuel cell EIS data for a) ELAT cathode and b) SS-CCE cathode.

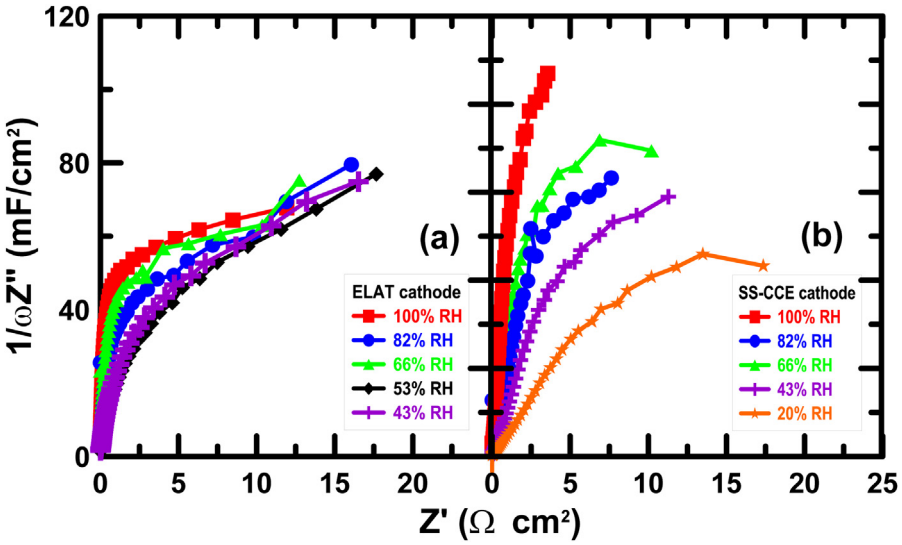

Fig. 7. Capacitance plots of fuel cell EIS data from a) ELAT cathode and b) SS-CCE cathode at 80 °C obtained with multiple cathode gas feed RH levels.

resistance within the catalyst layer, R_{Σ} as a function of RH [42]. Fig. 10 (a) and (b) display the R_{mem} and R_{Σ}, respectively, for the catalyst layers at each %RH. There is only a slight increase in membrane resistance as cathode %RH decreases, which indicates that the membrane is not severely afflicted by the change in water content. However, the ELAT MEA has consistently higher R_{mem} values than the SS-CCE cathode at each %RH. The ionic resistance, on the other hand, appears to be higher for the SS-CCE cathode than for ELAT. This result is not surprising as Nafion is well-established as an effective proton conducting ionomer.

Since water content within the membrane is crucial for proton conduction, the effects of variable %RH in the cathode on membrane resistance is a noteworthy result. The most common approach to increase tolerance to hot and/or dry conditions is to incorporate hygroscopic materials including SiO_2 [45–47] and even sulfonated silica [14,14,41,48–50] within the membrane. However, this does not necessarily facilitate hydration to the anode and cathode catalyst layers which results in lower fuel cell performance below 100% RH. Alternatively, our strategy was to utilize hygroscopic materials in the catalyst layer while maintaining a standard membrane. Considering both MEAs in the study were prepared with identical Nafion membranes and identical Pt/C electrocatalysts, it appears the addition of hygroscopic material within the cathode aids in maintenance of electrode activity while simultaneously hydrating the membrane. This is likely due to the back-diffusion of water from the cathode to the membrane [51]. Based on these findings, it is proposed that an MEA configured with hygroscopic materials at the electrodes may be a more optimal method to maintain fuel cell performance under dry or transient operating conditions. By employing the water retention agents in one or both electrodes their performance is maintained and hydration state of the membrane is maintained through enhanced transport of water from the catalyst layer(s) into the membrane. This may extend the range of operating conditions of MEAs prepared with standard membranes into drier/hotter conditions. However, it is not known at this time how water would freeze in an MEA prepared from a SS-

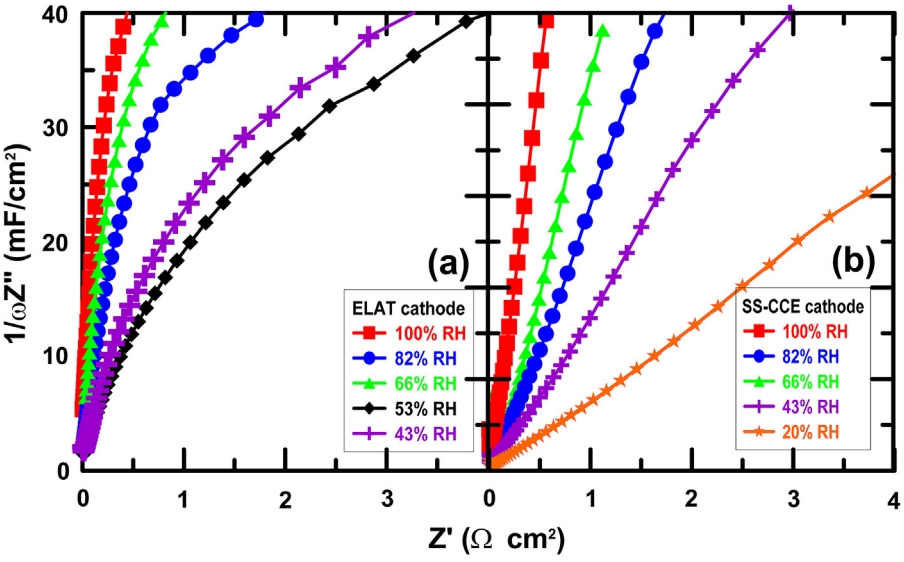

Fig. 8. Expansion of the high-frequency region for capacitance plots of fuel cell EIS data from a) ELAT cathode and b) SS-CCE cathode.

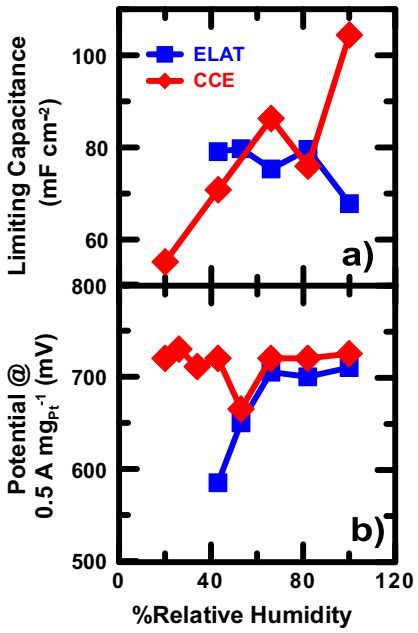

Fig. 9. a) Limiting capacitance and b) cell potential at 0.5 A mg_{Pt}^{-1} as a function of cathode gas feed RH for ELAT and SS-CCE cathodes at 80 °C.

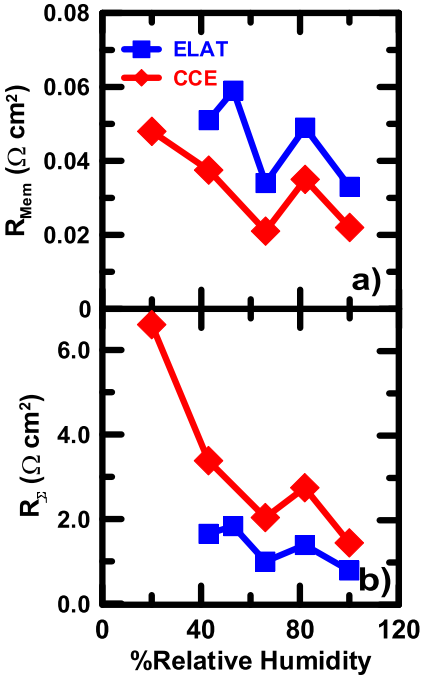

Fig. 10. a) Membrane resistance and b) total resistance as a function of cathode gas feed RH for ELAT and SS-CCE cathodes at 80 °C.

CCE and how this would impact the lower operating temperature of the MEA.

4. Conclusion

In this study, we have examined the physical and electrochemical characteristics of cathode catalyst layers including a Nafion-based cathode and a CCE-based cathode without Nafion. Our CCE-based catalyst layers appear to contain ca. 5% sulfonated silane of a total silane concentration of ca. 40%, which gives them their microporous structure. The addition of the small amount of sulfonated silane provides a source of proton conductivity without substantially changing microstructure or surface area as indicated from BET analysis. The use of silane materials did not result in a structure significantly different than a Nafion-based catalyst layer, as evidenced by TEM analysis of both the standard and CCE samples.

The CCE-based cathodes were able to maintain stable fuel cell performance down to 20% RH, and had especially better performance than the Nafion-based ELAT cathode. An increase in the ionic resistance of the CCE cathodes did not appear to have an effect on fuel cell performance. The use of identical Nafion membranes in the MEA, and the resulting decrease in membrane resistance for the CCE-based MEA, indicated that the presence of the sulfonated silane (TPS) in the cathode CL may aid in water retention and promote back-diffusion of water from the cathode to the membrane to improve MEA hydration. The hygroscopic nature of these Nafion-free catalyst layers suggests that they may be ideal candidates for use in low humidity operating conditions.

Acknowledgments

This work was supported by the Natural Sciences and Engineering Research Council (NSERC) of Canada through the Discovery Grants program, and UOIT. The authors thank Mike Strickland (Folio Instruments Inc.) for BET measurements, and Karolina Piorkowska (University of Western Ontario) for TEM images. JE acknowledges NSERC and OGS for scholarship support. The authors also thank Jesse Allan (UOIT) for providing FTIR spectra.

Appendix A. Supplementary data

Supplementary data related to this article can be found at http://dx.doi.org/10.1016/j.jpowsour.2013.07.005.

References

[1] G. Cacciola, V. Antonucci, S. Freni, J. Power Sources 100 (2001) 67–79.
[2] S. Litster, G. McLean, J. Power Sources 130 (2004) 61–76.
[3] E. Passalacqua, F. Lufrano, G. Squadrito, A. Patti, L. Giorgi, Electrochim. Acta 46 (2001) 799–805.
[4] J. Peron, Z. Shi, S. Holdcroft, Energy Environ. Sci. 4 (2011) 1575–1591.
[5] E.B. Easton, Z.G. Qi, A. Kaufman, P.G. Pickup, Electrochem. Solid State Lett. 4 (2001) A59–A61.
[6] J. Antonio Asensio, E.M. Sanchez, P. Gomez-Romero, Chem. Soc. Rev. 39 (2010) 3210–3239.
[7] A.W. Pedersen, A.D. Pauric, J.I. Eastcott, E.B. Easton, ECS Trans. 28 (2010) 39–49.
[8] C.Y. Du, T.S. Zhao, Z.X. Liang, J. Power Sources 176 (2008) 9–15.
[9] Y. Shao, J. Liu, Y. Wang, Y. Lin, J. Mater. Chem. 19 (2009) 46–59.
[10] Z. Xu, Z. Qi, A. Kaufman, Electrochem. Solid State Lett. 6 (2003) A171–A173.
[11] Z. Xu, Z. Qi, A. Kaufman, J. Power Sources 115 (2003) 49–53.
[12] Z. Xu, Z. Qi, A. Kaufman, Electrochem. Solid State Lett. 8 (2005) A313–A315.
[13] N. Lakshmi, N. Rajalakshmi, K. Dhathathreyan, J. Phys. D-appl. Phys. 39 (2006) 2785–2790.
[14] S. Sambandam, V. Ramani, J. Power Sources 170 (2007) 259–267.
[15] J. Peron, D. Edwards, A. Besson, Z. Shi, S. Holdcroft, J. Electrochem. Soc. 157 (2010) B1230–B1236.
[16] J. Park, P. Krishnan, S. Park, G. Park, T. Yang, W. Lee, et al., J. Power Sources 178 (2008) 642–650.
[17] T. Astill, Z. Xie, Z. Shi, T. Navessin, S. Holdcroft, J. Electrochem. Soc. 156 (2009) B499–B508.
[18] E.B. Easton, T.D. Astill, S. Holdcroft, J. Electrochem. Soc. 152 (2005) A752–A758.
[19] J. Muldoon, J. Lin, R. Wycisk, N. Takeuchi, H. Hamaguchi, T. Saito, et al., Fuel Cells 9 (2009) 518–521.
[20] S. von Kraemer, M. Puchner, P. Jannasch, A. Lundblad, G. Lindbergh, J. Electrochem. Soc. 153 (2006) A2077–A2084.
[21] E. Antolini, Appl. Catal. B Environ. 100 (2010) 413–426.
[22] T. Nakajima, T. Tamaki, H. Ohashi, T. Yamaguchi, J. Electrochem. Soc. 160 (2013) F129–F134.

[23] D. Banham, F. Feng, T. Fuerstenhaupt, K. Pei, S. Ye, V. Birss, J. Power Sources 196 (2011) 5438–5445.
[24] S. Zhang, L. Chen, S. Zhou, D. Zhao, L. Wu, Chem. Mat 22 (2010) 3433–3440.
[25] V.S. Velan, G. Velayutham, N. Hebalkar, K.S. Dhathathreyan, Int. J. Hydrogen Energy 36 (2011) 14815–14822.
[26] M.L. Anderson, R.M. Stroud, D.R. Rolison, Nano Lett. 2 (2002) 235–240.
[27] J.I. Eastcott, E.B. Easton, Electrochim. Acta 54 (2009) 3460–3466.
[28] H. Kim, P.A. Kohl, J. Power Sources 195 (2010) 2224–2229.
[29] A. Abbaspour, A. Ghaffarinejad, Electrochim. Acta 55 (2010) 1090–1096.
[30] B. Habibi, M.H. Pournaghi-Azar, Electrochim. Acta 55 (2010) 5492–5498.
[31] S. Ranganathan, E.B. Easton, Int. J. Hydrogen Energy 35 (2010) 1001–1007.
[32] S. Ranganathan, E.B. Easton, Int. J. Hydrogen Energy 35 (2010) 4871–4876.
[33] A. Abbaspour, E. Mirahmadi, Electrocatalytic hydrogen evolution reaction on microwave assisted sol-gel-derived carbon ceramic electrodes modified with metalophthalocyanines, J. Electroanal Chem. 652 (2011) 32–36.
[34] L. Rabinovich, O. Lev, Electroanalysis 13 (2001) 265–275.
[35] O. Lev, Z. Wu, S. Bharathi, V. Glezer, A. Modestov, J. Gun, et al., Chem. Mat. 9 (1997) 2354–2375.
[36] M. Tsionsky, G. Gun, V. Glezer, O. Lev, Anal. Chem. 66 (1994) 1747–1753.
[37] J.I. Eastcott, K.M. Yarrow, A.W. Pedersen, E.B. Easton, J. Power Sources 197 (2012) 102–106.
[38] T. Zawodzinski, T. Springer, F. Uribe, S. Gottesfeld, Solid State Ionics 60 (1993) 199–211.
[39] S. Ahn, Y. Lee, H. Ha, S. Hong, I. Oh, Electrochim. Acta 50 (2004) 673–676.
[40] J.I. Eastcott, J.A. Powell, A.J. Vreugdenhil, E.B. Easton, ECS Trans. 41 (2011) 853–864.
[41] N.E. De Almeida, E.B. Easton, ECS Trans. 28 (2010) 29–38.
[42] M.C. Lefebvre, R.B. Martin, P.G. Pickup, Electrochem. Solid State Lett. 2 (1999) 259–261.
[43] E.B. Easton, P.G. Pickup, Electrochim. Acta 50 (2005) 2469–2474.
[44] F.S. Saleh, E.B. Easton, J. Electrochem. Soc. 159 (2012) B546–B553.
[45] N. Miyake, J. Wainright, R. Savinell, J. Electrochem. Soc. 148 (2001) A898–A904.
[46] G. Ye, C.A. Hayden, G.R. Goward, Macromolecules 40 (2007) 1529–1537.
[47] M.P. Rodgers, Z. Shi, S. Holdcroft, J. Membr. Sci. 325 (2008) 346–356.
[48] Y. Kim, Y. Choi, H.K. Kim, J.S. Lee, J. Power Sources 195 (2010) 4653–4659.
[49] M. Lavorgna, M. Gilbert, L. Mascia, G. Mensitieri, G. Scherillo, G. Ercolano, J. Membr. Sci. 330 (2009) 214–226.
[50] M. Lavorgna, L. Mascia, G. Mensitieri, M. Gilbert, G. Scherillo, B. Palomba, J. Membr. Sci. 294 (2007) 159–168.
[51] M. Adachi, T. Romero, T. Navessin, Z. Xie, Z. Shi, W. Merida, et al., Electrochem. Solid State Lett. 13 (2010) B51–B54.